Available online at www.sciencedirect.com
ScienceDirect
Thermochimica Acta 459 (2007) 1–8
thermochimica acta
www.elsevier.com/locate/tca

Thermal stability and thermal decomposition study of hindered amine light stabilizers

A.I. Balabanovich [a,*], I.A. Klimovtsova [a], V.P. Prokopovich [a], N.R. Prokopchuk [b]

[a] *Research Institute for Physical Chemical Problems of the Belarusian State University, ul. Leningradskaya 14, 220030 Minsk, Belarus*
[b] *Belarusian State Technological University, ul. Sverdlova 13A, 220630 Minsk, Belarus*

Received 26 December 2006; received in revised form 17 March 2007; accepted 19 March 2007
Available online 24 March 2007

Abstract

The thermal decomposition of hindered amine light stabilizers for polyolefins based on bis(2,2,6,6-tetramethyl-4-piperidinyl) terephthalate (**I**), bis(2,2,6,6-tetramethyl-4-piperidinyl) *o*-phthalate (**II**) and 2,2,6,6-tetramethyl-4-piperidinyl stearate (**III**) has been studied using TG, DSC as well as FTIR of solid and GC/MS of high boiling decomposition products. The onset of weight loss in TG increases in the series: **III** < **II** < **I**. Ester cleavage by the β-elimination mechanism, scission of C–N bonds of the piperidine ring and aminolysis of the ester group have been shown to account for the formation of the decomposition products in the temperature range of 200–350 °C. The aminolysis reaction depresses the thermal stability of the studied compounds, in addition to the scission of the ester and C–N bonds. The yield of the products of aminolysis is higher from (**I**) and (**II**) compared to that from (**III**). The mass spectra of decomposition products and the decomposition scheme of the compounds under study are discussed.

Keywords: HALS; Thermal stability; Pyrolysis; Thermal analysis; FTIR

1. Introduction

Hindered amine light stabilizers (HALS) are commonly added to various polymeric materials in outdoor applications to prevent their photodegradation. They are composed of a secondary or tertiary cyclic amine unit and of a carboxylic acid component, and their function is ascribed [1] to radical scavenging by the nitroxide that can be formed by the oxidation of the HALS. In addition, HALS can be used as synergists to enhance flame retardancy of polymeric materials [2–4].

In order to be useful, any polymer additive must survive high temperatures used in the processing of polymeric materials (for instance, 250–270 °C for polyamides), therefore thermal stability studies of HALS are of importance. For example, a synthesis of more than 100 hindered piperidine compounds was reported [5], however only few were effective as light stabilizers, mainly because of poor thermal stability. This factor was likely to be a consequence for possible candidates for HALS to exhibit either high volatility or ability to decomposition resulting in the loss of their structure.

The development of HALS at the Research Institute for Physical Chemical Problems of the Belarusian State University has been a subject for many years [6,7], as there is a growing demand in stabilized polyolefin, polyester and polyamide polymers produced by the Belarusian industry. An important part of this work is studying thermal stability and thermal decomposition of the developed products, aimed at elucidation of the influence of the functional groups, the amine group or the ester group, on the loss of their structure. In this respect the work of Blazsó [8] is of importance, in which the effect of the ester group was shown in high temperature pyrolysis (400–900 °C) of HALS containing a tertiary amine group.

In addition, knowledge of decomposition products of HALS has to be taken into consideration, when plastic materials containing HALS are subjected to thermal recycling. It can be also used in sensitive and specific determination of HALS in

* Corresponding author. Tel.: +375 17 2095585; fax: +375 17 2264696.
E-mail address: balabanovich@bsu.by (A.I. Balabanovich).

0040-6031/$ – see front matter © 2007 Elsevier B.V. All rights reserved.
doi:10.1016/j.tca.2007.03.012

polymeric materials [9]. Our study contributes to these topics of pyrolysis chemistry.

2. Experimental

2.1. Materials

The objects of this study were a composition (HALS-1) of bis(2,2,6,6-tetramethyl-4-piperidinyl) terephthalate (**I**) (88% as determined by NMR spectroscopy), methyl 2,2,6,6-tetramethyl-4-piperidinyl terephthalate (10% by NMR) and dimethyl terephthalate (2% by NMR), which is an effective light stabilizer in polyolefins [5], bis(2,2,6,6-tetramethyl-4-piperidinyl) *o*-phthalate (**II**, HALS-2) and 2,2,6,6-tetramethyl-4-piperidinyl stearate (**III**, HALS-3), both with purity of about 97% (by NMR). They were prepared by transesterification reaction of either dimethyl terephthalate or dibutyl *o*-phthalate or ethyl stearate by 2,2,6,6-tetramethyl-4-piperidinol in *o*-xylene or dimethylformamide using a Lewis acid-type catalyst. HALS-1, -2, -3 were purified by precipitation with water from acetone solution. The yield of the synthesized products was of 85–95%. ^{1}H NMR of **I** (CD_3OD): δH = 8.07 (s, 4H, *p*-C_6H_4), 5.65–5.25 (m of nine lines, 2H, CH_2–*CH*–CH_2), 2.15–1.90 (dd, 4H, $(CH_3)_2C$–*CH*–CH), 1.60–1.35 (d, 4H, $(CH_3)_2C$–*CH*–CH), 1.35–1.10 (d, 26H, $(CH_3)_2C$ + NH) ppm. ^{1}H NMR of **II** ($CDCl_3$): δH = 7.80–7.40 (m, 4H, *o*-C_6H_4), 5.65–5.25 (m of nine lines, 2H, CH_2–*CH*–CH_2), 2.20–1.90 (dd, 4H, $(CH_3)_2C$–*CH*–CH), 1.40 (s, 2H, $(CH_3)_2C$–*CH*–CH), 1.35–1.05 (d, 30H, $(CH_3)_2C$ + $(CH_3)_2C$–*CH*–CH + NH) ppm. ^{1}H NMR of **III** ($CDCl_3$): δH = 5.40–5.00 (m of 9 lines, 1H, CH_2–*CH*–CH_2), 2.45–2.15 (t, 2H, CH_2–*CH*$_2$–CO), 2.05–1.65 (dd, 2H, $(CH_3)_2C$–*CH*–CH), 1.70–0.88 (m, 48H, CH_3 + CH_2 + NH) ppm. The NMR measurements were carried out using a TESLA BS-587A spectrometer operating at 80 MHz.

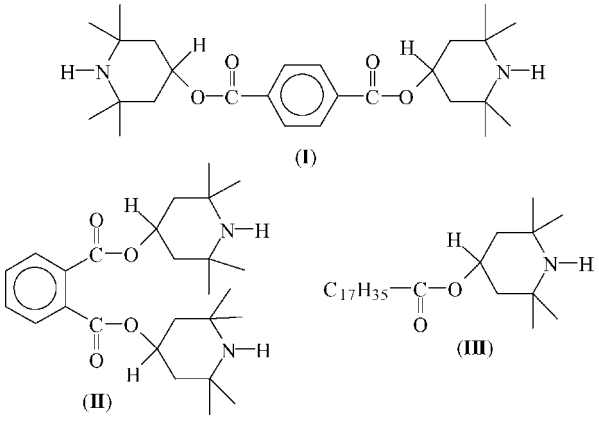

2.2. Thermal analysis

Thermal analysis was carried out using a Mettler TA 3000 thermal analyzer provided with a thermogravimetry (TG) module and a differential scanning calorimetry (DSC) cell. Standard measurements were performed at a heating rate of 10 °C min^{-1} under an argon flow of 60 cm^3 min^{-1}. The non-volatile fraction reproducibility was ±0.5%. The sample size was of about 10 mg.

2.3. Products of thermal degradation

For details of the thermal degradation procedure, the reader is referred to Ref. [10]. In short, high boiling decomposition products (HBPs) were collected under argon or helium in a degradation tube, the bottom part of which was hold at isothermal temperature 350 °C for 15 min, using samples of approximately 100 mg; whereas gaseous decomposition products were trapped at liquid nitrogen temperature and successively analyzed by GC/MS. The HBPs condensed in the upper part of the test tube were washed out by acetone, and the acetone solution was subsequently subjected to a GC/MS analysis (GC/MS model HP 6890/5972A) using a HP-1 60 m column which was temperature programmed from 50 °C (3 min) to 290 °C (20 min) at a heating rate of 10 °C min^{-1}. For analysis of gaseous products, the 60 m HP-1 capillary column was also found to be an appropriate column. The column was heated to 250 °C at a heating rate of 10 °C min^{-1} after an initial 3 min period at −40 °C. The mass spectra were obtained by electron ionization at 70 eV keeping the source at 180 °C. A mass spectrometric identification was carried out using Wiley and NBS libraries. In the few cases, when compounds were not included in the libraries, they were identified on the basis of both the molecular ion *m*/*z* value and of the ion decomposition pattern constructed for the best fit with the mass spectrum.

Solid residues collected at different steps of thermal decomposition in TG were investigated by IR spectroscopy on a Perkin Elmer "Spectrum 1000" FTIR spectrometer using KBr pellets.

3. Results and discussion

3.1. Thermal analysis

When heated at 10 °C min^{-1}, the studied HALS melt and exhibit an endothermal one stage weight loss process between 170 and 320 °C (Figs. 1 and 2). The onset temperature of weight loss (thermal stability) increases in the series HALS-3 < HALS-2 < HALS-1. The melting point temperature also increases in a similar way, i.e. 41 °C at HALS-3, 97 °C at HALS-2, and 204 °C at HALS-1. There was some black solid residue left after thermal decomposition (Fig. 1).

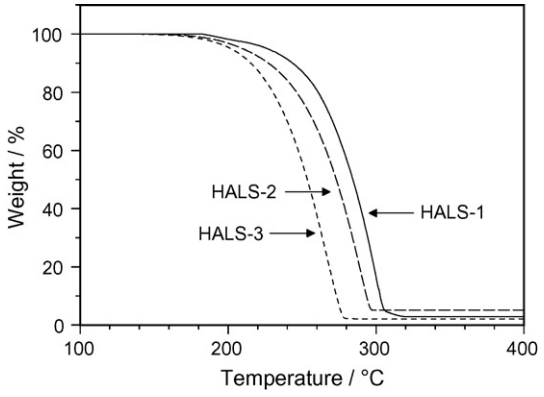

Fig. 1. Thermogravimetry of HALS-1, HALS-2, and HALS-3. Heating rate of 10 °C min^{-1} under nitrogen flow of 60 cm^3 min^{-1}.

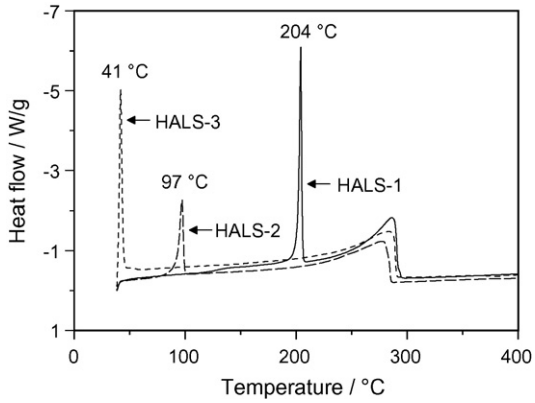

Fig. 2. DSC analysis of HALS-1, HALS-2, and HALS-3. Heating rate of 10 °C min^{-1} under nitrogen flow of 60 cm^3 min^{-1}.

3.2. FTIR study

The infrared spectra of the original HALS are presented in Fig. 3 (spectrum a) and Fig. 4 (spectra a and c), see also Table 1. The ester group of HALS-1 or -2 gives rise to the strong absorption bands at 1710 cm^{-1} due to the C=O stretching vibration, and two strong absorption bands at 1271 and 1122 cm^{-1} or 1294 and 1125 cm^{-1} due to the asymmetric and symmetric C–O–C stretching vibrations [11]. One of the strongest absorption bands in the FTIR spectra HALS-1 or -2 is the aromatic C–H deformation vibration located at 731 or 739 cm^{-1}. Because of the absence of conjugation with an aromatic ring, the ester C=O stretching vibration of HALS-3 absorbs at 1738 cm^{-1}, whereas the ester C–O–C stretching vibrations occur at 1235 and 1169 cm^{-1}. However, the most intense bands in the FTIR spectrum of HALS-3 are due to aliphatic C–H stretching vibrations

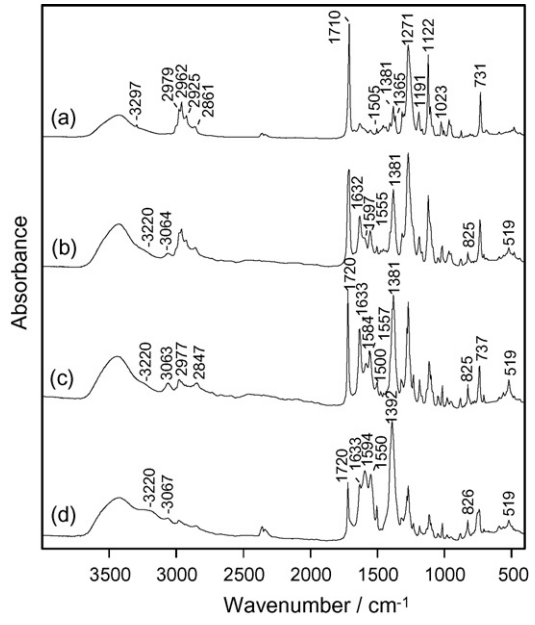

Fig. 3. Infrared spectra of initial HALS-1 (a) and solid products of its thermal decomposition collected in thermogravimetry at different steps of weight loss under inert atmosphere: 50% (b); 70% (c); at the end of the main stage of weight loss (d). Pellets in KBr.

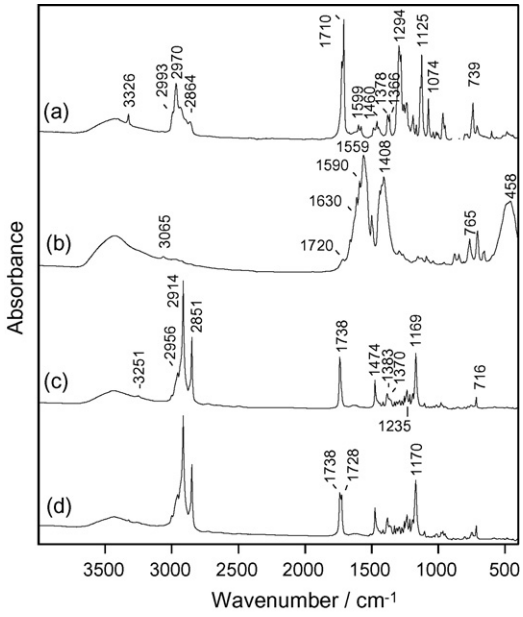

Fig. 4. Infrared spectra of initial HALS-2 (a) and HALS-3 (c) and solid products of their thermal decomposition collected in thermogravimetry under inert atmosphere at the end of the main stage of weight loss (b and d). Pellets in KBr.

of the methylene groups at 2914 and 2851 cm^{-1}; the deformation vibrations of the methylene group are located at 1474 and 716 cm^{-1}. The studied HALS are also characterized by a weak N–H stretching vibration of secondary amines between 3300 and 3250 cm^{-1}.

Thermal decomposition of HALS-1 resulted in a steadily decreasing intensity of the absorption bands at 1710, 1271 and 1122 cm^{-1} (spectra b–d) indicating decomposition of the ester structure. The aromatic band at 731 cm^{-1} declined as well. The profile of the C–H stretch spectral region at 2979–2861 cm^{-1} changed remarkably too. There was a significant decrease in the intensity and disappearance of the –CH_2-related bands. At the end of the main stage (spectrum d), only traces of the absorption bands due to CH_3 remained.

In addition, heating in the range of 220–320 °C resulted in the formation of new peaks at 3220, 1632, 1555 and 1381 cm^{-1} that increased in intensity up to 70% weight loss, after that the 1632 cm^{-1} peak declined. The peaks are characteristic of secondary amides (3220, 1632, 1555 cm^{-1}) and a carboxylate group (1555 and 1381 cm^{-1}) [11]. The residual absorption band at 1720 cm^{-1} (spectrum d) is indicative of an undecomposed

Table 1
Attribution of the main absorption bands of the studied HALS

Position: wavenumber (cm^{-1})			Attribution
HALS-1	HALS-2	HALS-3	
3297	3326	3251	ν(NH)
2979–2861	2993–2864	2956–2851	ν(CH)
1710	1710	1738	ν(C=O)
1381, 1365	1378, 1366	1383, 1370	δ(C(CH$_3$)$_2$)
1271, 1122	1294, 1125	1235, 1169	ν(C–O–C)
731	739	–	δ(C–H arom.)
–	–	716	δ(CH$_2$)

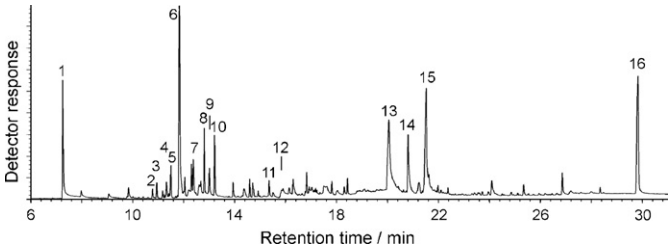

Fig. 5. Total ion gas chromatogram of the acetone-soluble HBPs of HALS-1 collected in the degradation apparatus at 350 °C. Peaks assignment in Table 2.

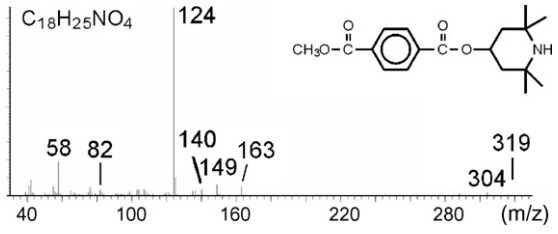

Fig. 7. Mass spectrum of methyl 2,2,6,6-tetramethyl-4-piperidinyl terephthalate (peak 16 in Fig. 5).

methyl terephthalate unite incorporated in the solid decomposition products, presented in the initial compound.

The FTIR spectra of the solid residues of HALS-2 and -3 showed little changes in the middle of thermal decomposition as the absorption bands of pyrolysis products appeared at the end of the main stage of weight loss. However, the FTIR spectrum of the sample of HALS-2 obtained at the end of pyrolysis (Fig. 4, spectrum b) resembles that of HALS-1 (Fig. 3, spectrum d), i.e. two strong broad absorptions around 1560 and 1400 cm^{-1} first of which being a superposition of the amide I, amide II bands, and the asymmetric CO_2^- stretching vibration [11]. The symmetric CO_2^- stretching vibration absorbs at 1400 cm^{-1} [11]. The carboxylate ion might be formed in the course of a reaction of the catalyst with phthalic acid structures. In addition, aromatic bands can be recognized at 3065, 1590 and 765 cm^{-1}.

The FTIR spectrum of the pyrolysis residue of HALS-3 obtained at 80% weight loss (Fig. 4, spectrum d) shows only an additional absorption band at 1728 cm^{-1} due to formation of an aliphatic acid structure.

3.3. GC/MS study

The total ion gas chromatogram of the HBPs of HALS-1 is shown in Fig. 5. The chromatographic peaks are assigned in Table 2. The mass spectra of the selected HBPs are shown in Figs. 6 and 7. The mass spectrum of 2,2,6,6-tetramethyl-1,2,5,6-tetrahydropyridine (peak 6 in Fig. 5) corresponds to that published in [8].

In Fig. 6 even mass numbers are indicative of a nitrogen-containing compound; therefore, the highest mass 84 is most likely attributed to a $(M - CH_3)^+$ ion. This points to the molecular mass of 99, which is consistent with the molecular formula $C_6H_{13}N$. The spectrum is dominated by the loss of 41, suggesting the presence of an allylic group. Taking into account the

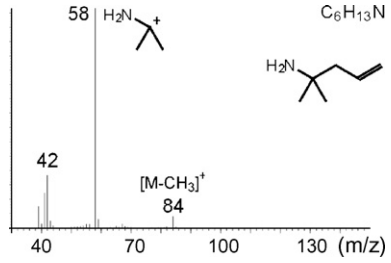

Fig. 6. Mass spectrum of 2-methylpent-4-en-2-amine (peak 1 in Fig. 5).

structure of the initial tetramethylpiperidinyl ring, the product is attributed to 2-methylpent-4-en-2-amine.

In Fig. 7 the mass spectrum shows many similarities with that of 2,2,6,6-tetramethyl-1,2,5,6-tetrahydropyridine, i.e. even mass numbers 42, 58, 82, and the most abundant mass 124, from which the presence of the tetramethylpiperidinyl ring is deduced in the unknown substance. In fact, the ring ion shows a weak peak at *m/z* 140 ($C_9H_{18}N^+$). The other support for the ring is the loss of the tetramethylpiperidinoxyl radical from the molecular ion, giving rise to the peak at *m/z* 163. The latter mass and that at *m/z* 149 are attributed to the *p*-$CH_3OOC–C_6H_4–CO^+$ and *p*-$HOOC–C_6H_4–CO^+$ ions correspondently. The mass spectrum is in accordance with the structure of methyl 2,2,6,6-tetramethyl-4-piperidinyl terephthalate.

The main HBPs from HALS-1 are 2-methylpent-4-en-2-amine, 2,2,6,6-tetramethyl-1,2,5,6-tetrahydropyridine, hydrocarbons C_9H_{14} which are likely to arise from decomposition of the piperidine ring, together with *p*-cyanobenzoic acid. The latter is generated from reaction involving the terephthalate unit [12]. Monomethyl terephthalate (15, Fig. 5) comes from decomposition of methyl 2,2,6,6-tetramethyl-4-piperidinyl terephthalate presented in the initial material. The formation of hydrocarbons C_9H_{14} is in accordance with the study [8] where an acyclic unsaturated hydrocarbon C_9H_{14} has been reported. FTIR examination of the HBPs revealed that some amounts of (**I**) evaporated.

The HBPs emitted during pyrolysis of HALS-2 are shown in Table 3, together with the relative area of the corresponding chromatographic peaks. As expected the main pyrolysis products are 2-methylpent-4-en-2-amine (product 1) 2,2,6,6-tetramethyl-1,2,5,6-tetrahydropyridine (product 2). The other important products are 2,2,6,6-tetramethyl-4-piperidinol (4) and 1,3-dimethyl-3-buten-1-yl *o*-cyanobenzoate (8) the structure of which is supported by the corresponding mass spectrum (Fig. 8). In fact, the molecular ion of (8) (*m/z* 229) shows three competitive losses of 147, 81, and 41 due to radicals of *o*-cyanobenzoic acid, $^{\bullet}C_6H_9$, and $^{\bullet}C_3H_5$. The first two losses give rise to ions at 82 ($C_6H_{10}^+$), and 148 (*o*-$NC–C_6H_4–C(OH)_2^+$ due to double hydrogen rearrangement). The latter ion exhibits successive eliminations of water and CO to give the *o*-$NC–C_6H_4^+$ ion at *m/z* 102.

The mass spectra of two other selected products evolved during pyrolysis of HALS-2 are presented in Figs. 9 and 10. The molecular ion of *N*-1,1-dimethylbut-3-en-1-ylbenzamide (Fig. 9) shows a loss of allylic radical producing ion at *m/z* 162. However, the most favourable decomposition pathway is

Table 2
HBPs emitted during pyrolysis of HALS-1

Entry	*m*/*z*	Relative area (%)	Structure
1	99	6	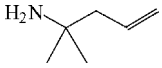
2, 3	122	<1	C_9H_{14}
4	106	<1	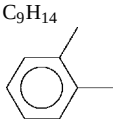
5	122	2	C_9H_{14}
6	139	3	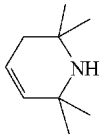
7	122	2	C_9H_{14}
8	120	3	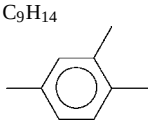
9	121	1	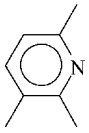
10	122	3	C_9H_{14}
11	139	1	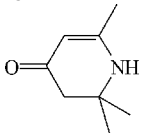
12	122	<1	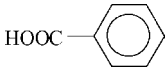
13	147	13	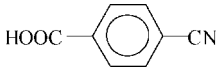
14	194	4	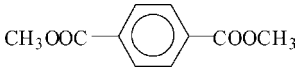
15	180	13	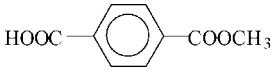
16	319	13	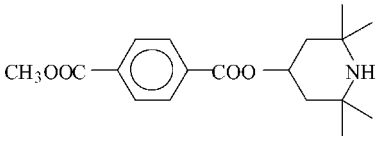

scission of the amide bond leading to the formation of ion at *m*/*z* 105 following by loss of CO to give ion at *m*/*z* 77.

The molecular ion of 1,3-dimethyl-3-buten-1-yl *N*-1,1-dimethyl-3-buten-1-ylphthalamate (Fig. 10) shows successive losses of the alkoxyl radical and 4-methylpentadiene to produce the $H_2NCO–C_6H_4–CO^+$ ion at *m*/*z* 148. The latter ion undergoes elimination of water from the amide group, which is accompanied by formation of ion at *m*/*z* 130.

The HBPs obtained during pyrolysis of HALS-3 are shown in Table 4. With respect to the area of the chromatographic peaks, the most important products are 2-methylpent-4-en-2-amine (1), 2,5-dimethylpyridine (2), 2,2,6,6-tetramethyl-1,2,5,6-tetrahydropyridine (3), octadecanitrile (22), octadecanoic acid (23), *N*-1,1-dimethylbut-3-en-1-yl-*n*-heptadecanamide (24). During pyrolysis HALS-3 volatilized too. The structure of amide (24) (Table 4) was deduced from its mass spectrum

Table 3
HBPs emitted during pyrolysis of HALS-2

Entry	*m*/*z*	Relative area (%)	Structure
1	99	10	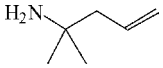
2	139	12	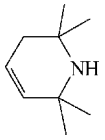
3	139	3	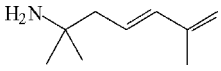
4	157	22	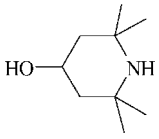
5	147	3	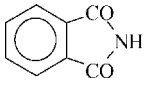
6	203	4	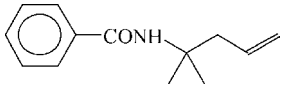
7	201	<1	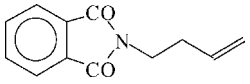
8	229	34	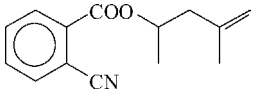
9	327	<1	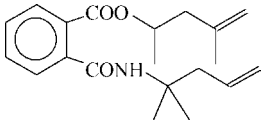
10	269	7	Not assigned

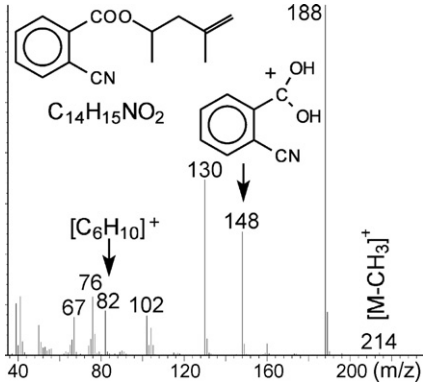

Fig. 8. Mass spectrum of 1,3-dimethylbut-3-en-1-yl *o*-cyanobenzoate (compound 8 in Table 3).

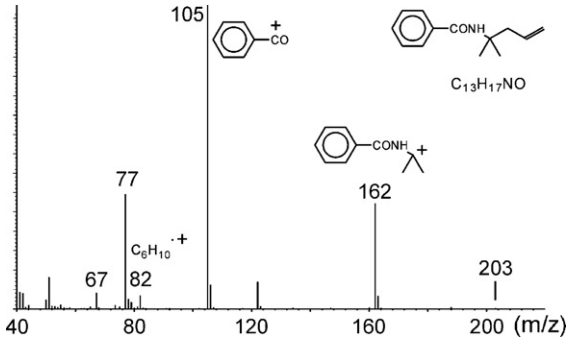

Fig. 9. Mass spectrum of *N*-1,1-dimethylbut-3-en-1-ylbenzamide (compound 6 in Table 3).

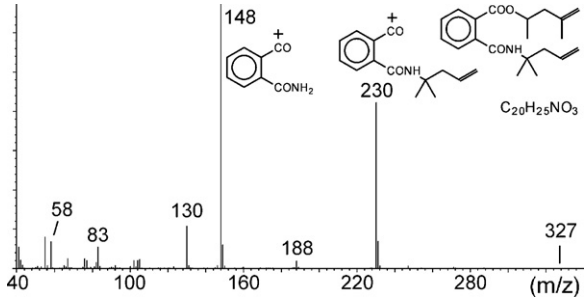

Fig. 10. Mass spectrum of 1,3-dimethyl-3-buten-1-yl *N*-1,1-dimethyl-3-buten-1-ylphthalamate (compound 9 in Table 3).

(Fig. 11) which is characterized by masses 324 and 284 originated from losses of the allylic and C_6H_9 (double hydrogen rearrangement) radicals. The loss of the $C_{16}H_{32}$ olefin from the acid side is observed as well, which results in the mass of the corresponding N-substituted acetamide at *m*/*z* 141. Appearance of the most abundant ion at *m*/*z* 58 (H_2N–$C(CH_3)_2^+$) can be understood by decomposition of the *m*/*z* 324 ion by breakdown of the amide CO–NH bond with a simultaneous H-transfer from the adjacent methylene group.

The total ion gas chromatogram of the gaseous products of HALS-1 is presented in Fig. 12. The main LBPs are acetone, 2-methyl-1,4-pentadiene and 2-methyl-1,3-pentadiene produced from decomposition of the piperidine ring. Pyrolysis of HALS-2 and -3 essentially resulted in the formation of the same products as they originate from fragmentations involving the piperidine ring.

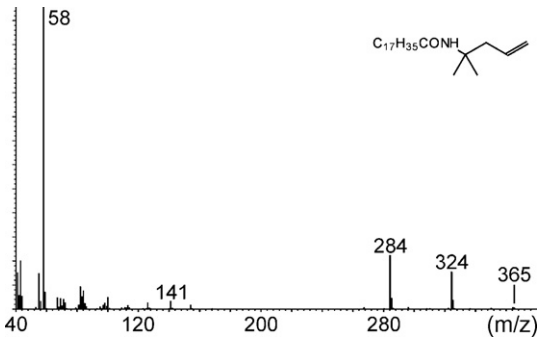

Fig. 11. Mass spectrum of *N*-1,1-dimethylbut-3-en-1-yl-*n*-heptadecanamide (compound 24 in Table 4).

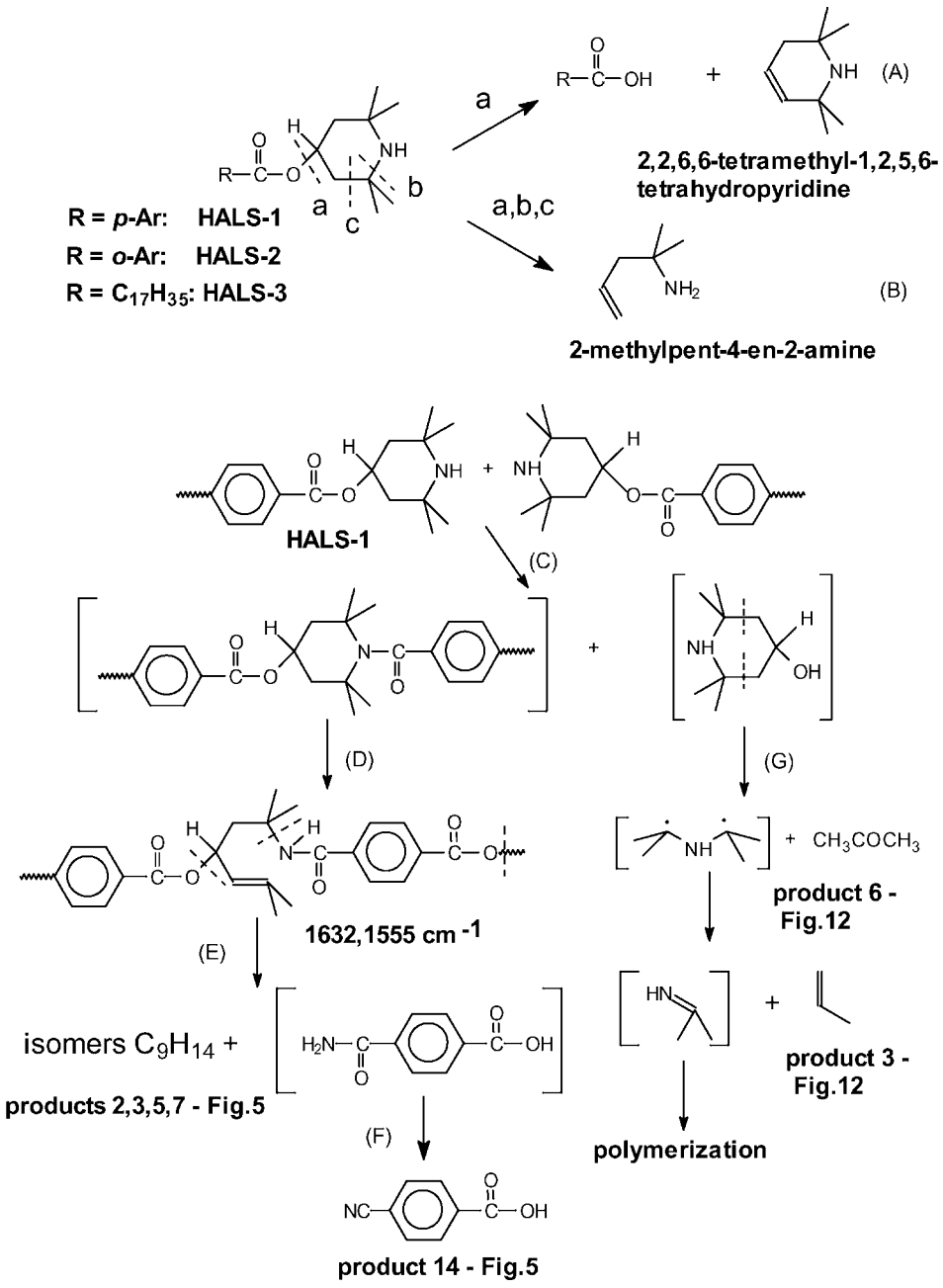

Scheme 1. Proposed decomposition scheme of the studied HALS compounds.

3.4. Proposed thermal decomposition scheme

FTIR and GC/MS studies show that the weight loss process in TG is due to evaporation and decomposition of HALS.

One of the reactions proposed for decomposition of HALS compounds is cleavage of the ester group by the β-elimination mechanism at the piperidine ring [8]. In the course of this reaction, the C–O bond labeled “a” breaks down and 2,2,6,6-tetramethyl-1,2,5,6-tetrahydropyridine is evolved from HALS-1, -2 and -3 (Scheme 1, path A). On the other hand, scission of the three bonds labeled “a”, “b”, and “c” results in the formation of 2-methylpent-4-en-2-amine (Scheme 1, path B).

In addition to these reactions, the present study revealed a new decomposition process resulting in the formation of secondary

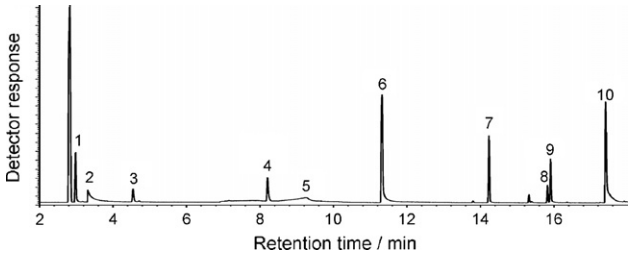

Fig. 12. Total ion gas chromatogram of the LBPs of HALS-1 collected in the degradation apparatus at 350 °C: (1) carbon dioxide; (2) ammonia; (3) propene; (4) 2-methylpropene; (5) water; (6) acetone; (7) 2-methyl-1,4-pentadiene; (8) 2-methyl-1,3-pentadiene; (9) 2-methyl-1,3-pentadiene; (10) 2-methylpent-4-en-2-amine.

Table 4
HBPs emitted during pyrolysis of HALS-3

Entry	*m*/*z*	Relative area (%)	Structure
1	99	6	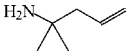
2	107	4	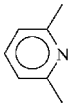
3	139	29	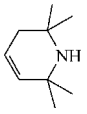
4	140	<1	*n*-$C_8H_{17}CH{=}CH_2$
5	142	<1	*n*-$C_{10}H_{22}$
6	154	<1	*n*-$C_9H_{19}CH{=}CH_2$
7	156	<1	*n*-$C_{11}H_{24}$
8	157	<1	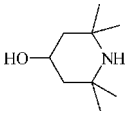
9	168	<1	*n*-$C_{10}H_{21}CH{=}CH_2$
10	170	<1	*n*-$C_{12}H_{26}$
11	182	<1	*n*-$C_{11}H_{23}CH{=}CH_2$
12	184	<1	*n*-$C_{13}H_{28}$
13	196	<1	*n*-$C_{12}H_{25}CH{=}CH_2$
14	198	<1	*n*-$C_{14}H_{30}$
15	210	<1	*n*-$C_{13}H_{27}CH{=}CH_2$
16	212	<1	*n*-$C_{15}H_{32}$
17	224	3	*n*-$C_{14}H_{29}CH{=}CH_2$
18	226	<1	*n*-$C_{16}H_{34}$
19	238	<1	*n*-$C_{15}H_{31}CH{=}CH_2$
20	240	2	*n*-$C_{17}H_{36}$
21	256	1	*n*-$C_{15}H_{31}COOH$
22	265	5	*n*-$C_{17}H_{35}CN$
23	284	32	*n*-$C_{17}H_{35}COOH$
24	365	8	n-$C_{17}H_{35}CONH$ 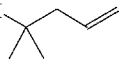
25	423	3	HALS-3

amides and nitrile-containing products. Obviously, the development of amides requires an interaction between an ester and an amine (aminolysis reaction), the reactive sites both existing in HALS. An additional aminogroup, the primary aminogroup, can be made up by decomposition of the piperidine ring (breakdown of a C–N bond). Both kind of aminogroups can be involved in the reaction with the estergroup, however, the product distribution does not give the clue which one is preferred. To illustrate the reaction scheme, we shall consider the transformation of the secondary aminogroup leading to the formation of a tertiary amide (Scheme 1, path C). A secondary amide the formation of which is especially pronounced in case of HALS-1 (Fig. 3) can be generated by scission of a C–N bond of the tertiary amide (path D). Further scission of the left C–N bond gives rise to nitriles (*p*-cyanobenzoic acid for HALS-1, 1,3-dimethylbut-3-en-1-yl *o*-cyanobenzoate for HALS-2, and octadecanitrile for HALS-3) as a result of the decomposition of primary amides due to dehydration (paths E and F) [13]. Their yield is higher for HALS containing aromatic ring compared to that for HALS-3 indicating that HALS-3 undergoes minor aminolysis.

In addition, the decomposition of the secondary amide can yield hydrocarbons C_9H_{14} (path E). Scheme 1 also suggests the formation acetone and propene by decomposition of 2,2,6,6-tetramethyl-4-piperidinol (path G) produced during the aminolysis reaction. A possible third product of this decomposition, an imine, is prone to undergo polymerization reactions [13].

4. Conclusions

The studied HALS-1, -2 or -3 are thermally stable additives to be introduced in polyolefins, however, they will volatilization during incorporation in polyamide-6. The decomposition reactions of the stabilizers mainly arise from the poor thermal stability and aminolysis of the ester bond, as well as from thermal fragmentations of the piperidine ring. The occurrence of aminolysis should be taken into consideration for development of new HALS as it may depress the thermal stability of HALS containing a secondary cyclic amine unit.

References

[1] J. Pan, Z. Yang, T. Zhang, W.W.Y. Lau, C.S. Lee, Polym. Deg. Stab. 44 (1994) 85–91.
[2] N. Capridinis, N. Lelly, PCT Patent Application WO 04/035673 (2004).
[3] D.W. Horsey, S.M. Andrews, L.H. Davis, D.D. Dyas Jr., R.L. Gray, A. Gupta, B.H. Hein, J.S. Puglisi, R. Ravichandran, P. Shields, R. Srinivasan, US Patent 6,599,963 (2003).
[4] N. Capridinis, G. Chandrika, J. Zing, PCT Patent Application WO 04/031286 (2004).
[5] K. Murayama, J. Synth. Org. Chem. (Japan) 31 (1973) 198–203.
[6] L.Yu. Smolyak, N.R. Prokopchuk, V.P. Prokopovich, I.A. Klimovtsova, Doklady NAN Belarusi 42 (1998) 65–68 (in Russian).
[7] V.P. Prokopovich, I.A. Klimovtsova, N.R. Prokopchuk, L.Yu. Smolyak, Belarus Patent 5349 (2003).
[8] M. Blazsó, J. Anal. Appl. Pyrolysis 58–59 (2001) 29–47.
[9] Y. Taguchi, H. Ohtani, S. Tsuge, Y. Ishida, K. Kimura, T. Yoshikawa, J. Chromatogr. A 993 (2003) 137–142.
[10] A.I. Balabanovich, J. Fire Sci. 21 (2003) 285–298.
[11] G. Socrates, Infrared and Raman characteristic group frequencies, in: Tables and Charts, 3rd ed., John Wiley & Sons, Chichester, 2004.
[12] A.I. Balabanovich, A.M. Balabanovich, J. Engelmann, Polym. Int. 52 (2003) 1309–1314.
[13] M.B. Smith, J. March, March's Advanced Organic Chemistry: Reactions, Mechanisms and Structures, John Wiley, New York, 2001.